Soliton communication beyond the average-soliton regime

R.-J. Essiambre and Govind P. Agrawal

The Institute of Optics, University of Rochester, Rochester, New York 14627-0186

Received May 26, 1995; revised manuscript received July 31, 1995

We study semianalytically soliton dynamics in a soliton-based communication line for which the amplifier spacing is larger than the soliton period (referred to as the quasi-adiabatic regime). This regime allows us to overcome the limit on the soliton duration ($T_{\mathrm{FWHM}} \sim 15$ ps) imposed by the average-soliton regime. Our calculations show that periodically stable propagation of short solitons ($T_{\mathrm{FWHM}} = 1-5$ ps) is possible for an amplifier spacing ranging from 5 to 20 km. We discuss the dynamical features associated with the propagation of short solitons in the quasi-adiabatic regime and present a simple model capable of predicting the width and the mean frequency of the steady-state soliton. We compare the model with appropriate numerical simulations. Our analysis may also be applied to fiber lasers that produce ultrashort solitons ($T_{\mathrm{FWHM}} < 1$ ps) in a relatively long-cavity configuration.

1. INTRODUCTION

Soliton-based communication systems are attracting considerable attention because of their potential for transmitting high-bit-rate signals over transoceanic distances. Because of intrinsic fiber losses, solitons lose energy continuously, and the energy loss become significant for distances > 10 km. A continuous compensation of these losses has been realized through the use of distributed amplification in long active fibers.[1,2] But, until now, transmission schemes based on distributed amplification have not been practical. Of course, one can also compensate for fiber losses by periodic amplification of solitons by placing equally spaced fiber amplifiers along the transmission link. In such a case, the nonlinear Schrödinger equation (NSE) with distributed loss and periodic amplification can be transformed into a new NSE for the averaged soliton amplitude with an additional term proportional to the square of the ratio of the amplifier spacing to the soliton period.[3,4] For this term to be a small perturbation, the amplifier spacing must be much smaller than the soliton period. In such a case, even if the soliton experiences significant losses between two amplifiers its average parameters are still described by the NSE. Inasmuch as the soliton period is proportional to the square of the soliton width, the condition for realizing an average soliton leads to a lower limit on the soliton duration for practical amplifier spacings. This limit is approximately $T_{\mathrm{FWHM}} = 15$ ps for an amplifier spacing of 30 km in a dispersion-shifted fiber having an anomalous dispersion of -1 ps^2/km. One can reduce it slightly when the soliton period approaches the amplifier spacing by making use of nonlinear compression. This scheme is known as dynamic soliton communication[5] because of the use that it makes of the dynamic range of soliton stability. In such a regime the average pulse propagating in the fiber is no longer a first-order soliton but rather a soliton having a peak power between a first- and a second-order soliton. However, without any form of soliton control the periodic amplification scheme becomes unstable over multiple amplifier stages when the peak power of the input soliton is too large.[6]

Soliton communication systems operating at bit rates > 20 Gb/s generally require soliton pulses of widths < 10 ps to minimize the mutual interaction between neighboring solitons. Numerical simulations show that, when such short solitons propagate over several amplification stages, dispersive waves are generated that resonantly interact with the solitons, undermining their stability.[7,8] Clearly, the average soliton dynamics description is not appropriate for modeling the propagation of short solitons ($T_{\mathrm{FWHM}} = 1-5$ ps) for typical amplifier spacings of 20–30 km. In this paper we study the conditions under which short solitons of 1–5 ps width can be propagated stably over large distances. It so happens that in low-loss silica fibers such short solitons have soliton periods that are not only smaller than a typical amplifier spacing (~20–30 km) but also smaller than the characteristic loss length (distance over which 50% of the power is lost, ~15 km). In such a case the parameters describing the soliton can be considered as evolving slowly because the soliton reshapes itself continuously during the propagation to follow the losses. For this reason we refer to soliton dynamics as quasi-adiabatic in this paper. The quasi-adiabatic regime is defined as the regime in which the soliton period is smaller than the amplifier spacing because in optical fibers both the loss length and the typical amplifier spacing are of the same order. Solitons propagating in this regime are called short solitons for simplicity.

The main phenomena that occur during the propagation of short solitons in a communication line can be summarized as follows. First, the soliton evolves over many soliton periods, permitting soliton broadening and nonlinear pulse compression on a scale shorter than the amplifier spacing. Second, this dynamical evolution increases the energy spread in the form of dispersive waves, which may enhance resonant instabilities associated with the copropagation of dispersive waves and solitons. Third, the intrapulse Raman scattering becomes significant, and so does, to a lesser extent, the (linear) third-order dis-

0740-3224/95/122420-06$06.00

persion. Fourth, effects of the limited bandwidth of the gain may become important and may even be necessary to cancel the Raman-induced frequency shift. Our numerical simulations have shown that the effects of intrapulse Raman scattering and the resonant instabilities are the most harmful effects that need to be addressed before short solitons can be used for communication purposes. In particular, if it is not controlled, the effect of the intrapulse Raman scattering will be to shift the soliton to frequencies at which the group-velocity dispersion can be considerably different from its value at the frequency of the input soliton. Such a change in the conditions of propagation together with the resonance of dispersive waves with the soliton eventually results in the destruction of the soliton bit stream and the loss of information content.

2. MODEL

We present in Fig. 1 a schematic of the communication line considered. The two main elements are a limited-bandwidth amplifier and a fast saturable absorber (FSA).[9] The former element (alone or in combination with a frequency filter) is used to compensate for the downward frequency shift of solitons (the soliton self-frequency shift[10], SSFS) associated with the intrapulse Raman scattering. Such compensation is possible only if the gain (filter) bandwidth approaches the soliton spectral width. The FSA has been introduced to reduce the resonant instabilities[11] and to prevent the production of secondary solitons.[12] To illustrate the importance of a FSA, we show in Fig. 2(a) the evolution of a 4.5-ps soliton over eight amplification stages in absence of FSA. Figure 2(b) presents the same simulation over 51 amplification stages when a FSA is inserted at every amplifier, allowing a periodic regime to settle. The amplifier spacing is 20 km in both cases. In the quasi-adiabatic regime, because the soliton period ($z_s = \pi L_D/2$ with the dispersion length $L_D = T_p^2/|\beta_2|$, where T_p is the soliton width) is smaller than the amplifier spacing z_a, the dispersive waves, generated because of nonideal soliton propagation, spread significantly over one stage. A FSA-type element can remove these waves efficiently in this regime without perturbing the soliton too much.[13] It is worth noticing that the effects of a FSA-type element on the accumulation of dispersive waves created by filtering have been studied in the context of the average soliton.[14] Such an element has been shown to lead to a reduction of resonant effects between dispersive waves and the soliton simultaneously with a reduction of the Gordon–Haus effect.[15] Because of the relatively low rate of emission of the dispersive waves in the average-soliton regime, the period of insertion of the FSA was of the order of 1000 km.

Unlike in the average-soliton regime, the propagation of short solitons can hardly be described in terms of averaged parameters mainly because, in addition to such solitons' having large variations in amplitude (and hence in width), their mean frequency is likely to change considerably over one amplifier spacing. One can then obtain the steady-state conditions by studying a two-dimensional map formed by the soliton amplitude and the mean frequency. The mapping relates the soliton amplitude and the mean frequency at one amplifier to their values at the previous amplifier. The special case in which the two-dimensional map can be reduced to one dimension in presence of dispersive losses has been considered analytically.[16] In this paper we numerically solve the two equations that together form a two-dimensional map describing the soliton energy (equivalent to the soliton amplitude in the adiabatic approximation) and the mean frequency by imposing periodic conditions of propagation.

The first and obvious condition of periodicity is that all losses within one stage be compensated for by the lumped gain. However, unlike in the average-soliton regime, a second condition appears for short solitons because the SSFS can be larger by more than 4 orders of magnitude for such a case [see Eq. (7) below]. This frequency shifting should be compensated for stability. This leads to the second condition that the downward shift of the soliton mean frequency be periodically compensated for by an appropriate upward frequency shift (we are not considering here the case of sliding-frequency filters).[17] For lumped amplification, significant upward frequency shifts at the amplifier can be accomplished only when the gain (or filter) bandwidth becomes close to the soliton spectral width. Thus the effects of bandwidth-limited amplifica-

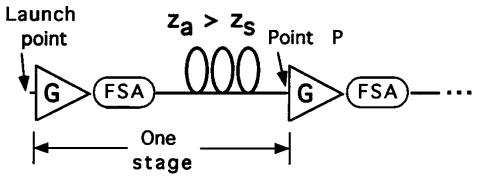

Fig. 1. Schematic of the proposed transmission line. The amplifier spacing z_a can be larger than the soliton period z_s. G's, amplifier gain.

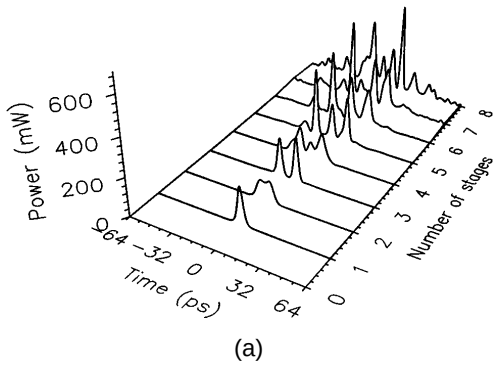

(a)

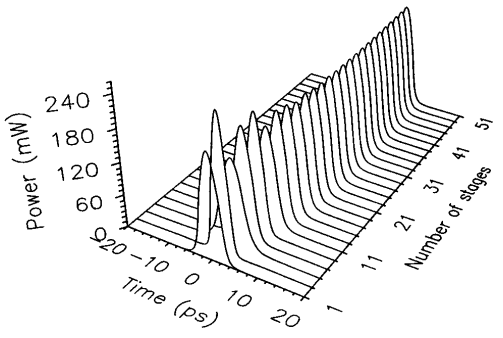

(b)

Fig. 2. Comparison of soliton evolution (a) without and (b) with a FSA. The amplifier spacing is 20 km and the soliton width (FWHM) is 4.5 ps.

tion need to be carefully addressed when one is modeling short-soliton communication systems. For the sake of generality, no approximations are made about the form of the amplifier spectrum for the calculations.

As mentioned above, we look for the steady-state evolution of a periodically amplified short soliton by considering the soliton's amplitude and mean frequency just before the amplifier (point P in Fig. 1). The steady-state conditions can be written as

$$G(\nu_0, u_0)\, L = 1\,, \tag{1}$$

$$\Delta\nu_{\mathrm{amp}}(\nu_0, u_0) + \Delta\nu_{\mathrm{SSFS}}(u_0) = 0\,, \tag{2}$$

where G and L are the amplification and the loss, respectively, during one stage and $\Delta\nu_{\mathrm{amp}}$ and $\Delta\nu_{\mathrm{SSFS}}$ represent the frequency shifts associated with the amplification process and the intrapulse Raman scattering, respectively. We find the stable soliton characteristics by solving Eqs. (1) and (2) for the soliton amplitude u_0 and the mean frequency ν_0.

The amplification factor G corresponds to the relative gain in energy at the amplifier and is evaluated by the following integrals in the frequency domain:

$$G(\nu_0, u_0) = \frac{\int_{-\infty}^{\infty} G_L(\nu)\,|v(\nu)|^2\,\mathrm{d}\nu}{\int_{-\infty}^{\infty} |v(\nu)|^2\,\mathrm{d}\nu}\,, \tag{3}$$

where $G_L(\nu)$ is the amplifier spectrum and $v(\nu)$ is the soliton spectrum at point P. The fundamental soliton[18] is represented by $u(\tau) = u_0\ \mathrm{sech}(u_0\tau)\exp[-i\,2\,\pi\,\nu_0\,\tau]$, where $\tau = T/T_0$ is the normalized time (T_0 is a normalization constant and T the running time), and ν_0 accounts for a shift of the soliton mean frequency from the carrier frequency. All frequencies are measured with respect to the gain peak of the amplifier. The soliton width is given by $T_{\mathrm{FWHM}} = 1.763/u_0$. We have neglected phase terms not dependent on τ and the frequency-dependent time shift when writing $u(\tau)$ because they do not modify the results of our analysis. We note that the two parameters u_0 and ν_0 are necessary for a unique definition of the soliton. The soliton spectrum is given by $v(\nu) = \pi\ \mathrm{sech}[\pi^2(\nu - \nu_0)/u_0]$ with the spectral width (FWHM) $1.763\,u_0/\pi^2$.

Consider first the case of an amplification stage consisting of a homogeneously broadened gain medium with a Lorentzian gain spectrum:

$$G_L(\nu) = L_I\ \exp\{\, g_0 \,/\, [1 + (\nu/\Delta\nu_G)^2]\}\,, \tag{4}$$

where g_0 is the unsaturated gain coefficient and $\Delta\nu_G$ is the gain bandwidth and where we have included in the effective gain G_L a transmission factor L_I that accounts for insertion loss when the energy is coupled to the fiber. The loss factor L in Eq. (1) that represents the fraction of energy left in the soliton after propagation in the fiber and through the FSA can be written as

$$L = \exp(-\alpha z_a)(1 - L_{\mathrm{FSA}})\,, \tag{5}$$

where α represents distributed fiber losses and has a value of 0.04835 km^{-1} for a loss of 0.21 dB/km, z_a is the amplifier spacing, and L_{FSA} represents the energy loss through the FSA (normalized to the soliton energy).

We evaluate the frequency shift imposed by the amplifier by taking the first moment of the power spectrum of the amplified soliton, and it is given by

$$\Delta\nu_{\mathrm{amp}}(\nu_0, u_0) = \frac{\int_{-\infty}^{\infty} \nu\ G_L(\nu)\,|v(\nu)|^2\,\mathrm{d}\nu}{\int_{-\infty}^{\infty} G_L(\nu)\,|v(\nu)|^2\,\mathrm{d}\nu}\,. \tag{6}$$

The expression for the SSFS associated with the Raman effect is derived from the formula for an ideal fundamental soliton[10,19]:

$$\frac{\partial\nu_0(z)}{\partial z} = -\frac{4}{15\pi}\,\frac{T_R}{T_0}\,\frac{1}{\tau_p{}^4(z)}\,, \tag{7}$$

where z is the normalized distance, T_R is a characteristic time (chosen to be 6 fs), T_0 is the normalization time set to 1 ps, and $\tau_p(z)$ is the normalized soliton width, which, unlike in the average soliton regime, depends on the position of the soliton in the fiber. One can relate the soliton width at the end of one stage to the soliton width of the amplified soliton launched into the fiber by considering energy losses. Because the soliton evolves in the fiber with a relatively low loss per soliton period, we assume that the soliton width growth rate is inversely related to the rate of decay of the soliton energy:

$$\tau_p(z) = \tau_p(0)\exp(\alpha z)\,. \tag{8}$$

By replacing Eq. (8) in Eq. (7), integrating over the fiber length z_a, and expressing the result in terms of the soliton width at $z = z_a[\tau_p(z_a) = 1/u_0]$ we obtain

$$\Delta\nu_{\mathrm{SSFS}}(u_0) = \frac{T_R\,[1 - \exp(4\,\alpha z_a)]}{15\pi\alpha T_0}\,u_0{}^4\,, \tag{9}$$

which expresses the value of the SSFS in terms of the soliton amplitude at point P for different amplifier spacings. Equation (9) can also be derived through adiabatic perturbation theory.[16]

It is worth noticing that our numerical simulations show that a nonlinear compression generally occurs in the first part of the fiber, indicating that the amplified pulse entering the fiber is not an exact fundamental soliton. But this effect is small enough (typical compression ratios between 1.2 and 1.6) that Eq. (8) can represent the evolution of the average soliton width and Eq. (9) remains quite accurate when compared with numerical simulations.

When communication lines of different amplifier spacings are considered, the gain peak $G_0 \equiv G_L(\nu = 0)$ must be adjusted to compensate for different fiber losses and thus depends on the amplifier spacing z_a through the relation

$$G_0(z_a) = \frac{E_G\ \exp(\alpha z_a)}{1 - L_{\mathrm{FSA}}}\,, \tag{10}$$

where we include an excess gain factor E_G in addition to the loss compensation because, in general, the soliton spectrum is not small compared with the gain bandwidth and the mean frequency of the soliton does not coincide with the central frequency of the gain, leading to a reduced effective gain compared with the peak gain G_0. The last parameter to be set (L_{FSA}) represents losses through a FSA, which in general depend on the propaga-

tion of the perturbed soliton and the type of FSA used. We numerically observed that L_{FSA} is an increasing function of distance (as it is related to the emission of dispersive waves), but we fixed it to 0.05 for simplicity.

3. RESULTS

We now solve the coupled set of Eqs. (1) and (2) for ν_0 and u_0, using Eqs. (3), (5), (6), and (9). Inasmuch as Eqs. (1) and (2) are not easily solvable analytically under general conditions, we present here numerical solutions of these equations.

We first consider the case of different amplifier spacings with the gain bandwidth $\Delta\nu_G$ fixed to $1/\pi$ THz (of the order of the spectral width of a 1-ps soliton). Figure 3 shows the steady-state soliton width and the mean frequency for three different situations: (i) a Lorentzian gain spectrum with 50% insertion losses ($L_I = 0.5$), (ii) a Lorentzian gain spectrum without insertion losses ($L_I = 1$), and (iii) a large-bandwidth gain spectrum in combination with an optical filter, i.e., $G_L(\nu) \rightarrow G_L(\nu)|H(\nu)|^2$, where $H(\nu) = 1/(1 + i\nu/\Delta\nu_F)$ and $\Delta\nu_G \gg \Delta\nu_F$. These three effective gains have the same gain peak, and their bandwidths are adjusted to provide the same amplification to a 1-ps soliton centered at the gain peak for a given amplifier spacing. Note that we neglect dispersion and nonlinear effects within the amplifier because of the small length (~10 m) of a typical amplifier compared with the soliton period (>1 km).

Figure 3(a) shows the steady-state soliton width as a function of the amplifier spacing for the three effective gain models, and Fig. 3(b) shows the corresponding mean frequencies. The peak gain G_0 is adjusted for the different amplifier spacings according to Eq. (10) with $E_G = 1.4$. As may be expected, the mean frequency of the soliton is shifted to lower frequencies to receive an upward frequency shift at every amplifier. As we increase the amplifier spacing, broader solitons are predicted, allowing the SSFS to be low enough to keep the soliton within the amplifier spectrum. It is worth noting that the shift of the soliton mean frequency is relatively small for the Lorentzian gain spectrum with 50% insertion loss or when a bandpass filter is inserted in the line. However, a much larger frequency shift occurs in the absence of insertion losses. This suggests that insertion losses may play an important role in the frequency stabilization of periodically amplified short solitons if bandpass filters are not used.

The influence of the value of the gain bandwidth on the soliton duration is presented in Fig. 4 for two effective gains. Figure 4(a) shows the steady-state soliton width for different gain bandwidths for the Lorentzian gain spectrum with loss [case (i)] for three different amplifier spacings. For amplifier spacings of 10 and 15 km, the steady-state soliton durations range from 1.5 to 3 ps, whereas for an amplifier spacing of 20 km the range of bandwidth to generate short solitons is reduced. Figure 4(b) shows the soliton width for case (iii) (insertion of a bandpass filter). Similar results are obtained for an amplifier spacing of 10 or 15 km, but, clearly, for a large amplifier spacing the bandwidth must be reduced to produce the shortest pulses. However, numerical simulations show that, for such a filtering scheme, more energy is lost through emission of dispersive waves, which reduces the effectiveness of this configuration. This may be due to the strong spectral reshaping introduced by the filter [contrary to the case of Fig. 4(a), the filter is opaque outside the bandpass window], leading to an increase in the generation of dispersive waves.

Figure 5 compares the results obtained by solution of Eqs. (1) and (2) with those obtained by numerical integration of the generalized NSE:

$$\frac{\partial u}{\partial z} + \frac{i}{2}\beta_2\frac{\partial^2 u}{\partial t^2} - i|u|^2u = -\frac{\alpha}{2}u - T_R u\frac{\partial |u|^2}{\partial t} + \frac{\beta_3}{6}\frac{\partial^3 u}{\partial t^3}, \tag{11}$$

where standard notation has been used.[18] The parameters $\alpha = 0.21$ dB/km and $T_R = 6$ fs have the same values in both cases. We have included the third-order dispersion in the numerical simulations for completeness by choosing $\beta_3 = 0.1$ ps^3/km. Our simulations have shown that the third-order dispersion accounts for a very small frequency shift (2 orders of magnitude smaller than

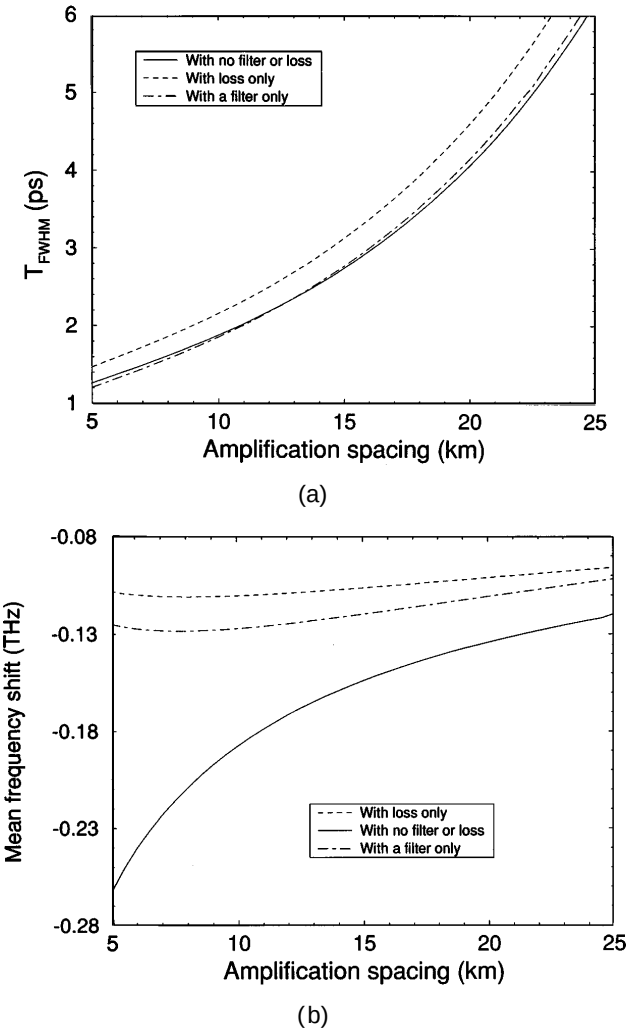

Fig. 3. Steady-state (a) soliton width and (b) mean frequency shift for different effective gain models. (i) Solid curve, a Lorentzian amplifier spectrum with 50% insertion losses; (ii) short-dashed curve, a Lorentzian amplifier spectrum without insertion losses; (iii) long-and-short-dashed curve, a large-bandwidth amplifier spectrum with a narrow-bandwidth bandpass filter.

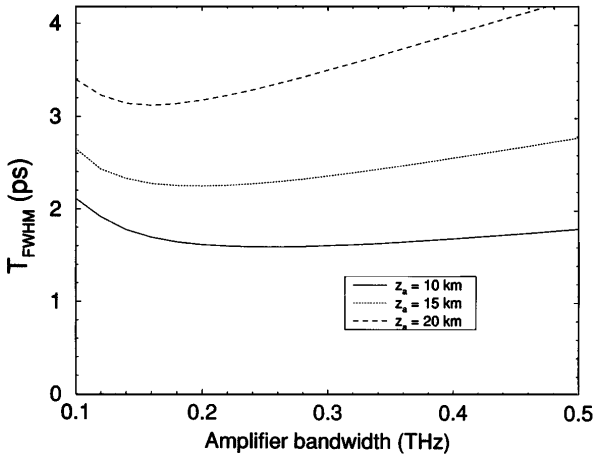

(a)

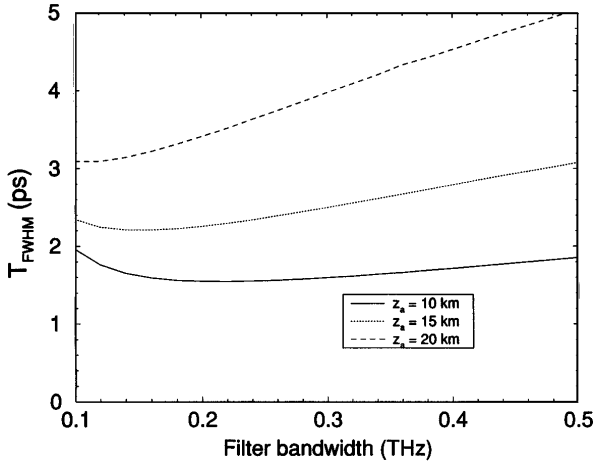

(b)

Fig. 4. Steady-state soliton width plotted as a function of the gain bandwidth for three different amplifier spacings: (a) a Lorentzian amplifier spectrum with 50% insertion losses and (b) a large-bandwidth amplifier spectrum with a narrow-bandwidth bandpass filter.

the SSFS). The saturation power of the FSA has been fixed to ~50 mW for every simulation so that the ratio of the saturation power to the soliton peak power ranges from 2% to 30% depending on the amplifier spacing. The energy loss through the FSA is evaluated numerically for each amplifier spacing and used in the semianalytic calculations. The differences between numerical results and solutions of Eqs. (1) and (2) are attributed mainly to the fact that we have neglected energy losses through emission of dispersive waves when writing the evolution of the average soliton width [Eq. (8)]. As expected, larger discrepancies are observed for large amplifier spacings because more dispersive waves are generated.

4. DISCUSSION AND CONCLUSION

We found numerically that the limit of the validity of the model presented in this paper is settled by the maximum energy gain that can be provided to a soliton without inducing a fission of solitons.[12] We estimate this maximal value of G to be ~2.8, which puts a limit of ~23 km on the amplifier spacing. This limit is fixed by the fiber loss and could be increased by the development of very low-loss fibers in contrast to the amplification spacing of the average-soliton regime, which depends on the width of the propagating soliton. We also numerically observed that in some cases, although a stable solution exists, it cannot be reached through an input soliton of mean frequency centered at the peak gain because soliton fission occurs before the steady state is achieved. These cases correspond to regimes in which the effective gain is near the critical value at which the generation of multiple solitons occurs. We can understand this splitting by considering that, at steady state, because of the offset between the soliton mean frequency and the gain central frequency, the effective gain received by a soliton is less than that which occurred when both frequencies were equal. Thus, near the critical gain value, a soliton will not generate secondary solitons if its mean frequency is close to the steady-state value but may undergo soliton splitting if its frequency lies in the region near the gain peak. Operation of a communication line near the critical gain value (hence for large amplifier spacings) may thus require tuning of the input soliton in a proper frequency range [downshifted from the gain peak; see Fig. 3(b)]. Numerical simulations indicate that an increase in the saturation power of the FSA may, to a certain extent, prevent the generation of secondary solitons. As these parasitic solitons are usually of low power, the FSA absorbs sufficiently of their energy to inhibit their growth. However, as the saturation power increases, less energy pass through the FSA, resulting in no stable pulse transmission for a saturation power too large.

The existence of solutions of the set of Eqs. (1) and (2) does not guarantee their stability, but numerical simulations have shown a range of stability for various soliton peak powers. We can understand this by noting that a soliton of higher energy will experience a larger frequency shift and will thus receive lower gain at the next amplifier, reducing its excess energy. A similar negative feedback applies to solitons of low energy. On the other hand, for some gain parameters the soliton energy oscillates periodically, which is typical of the dynamics of a nonlinear system.

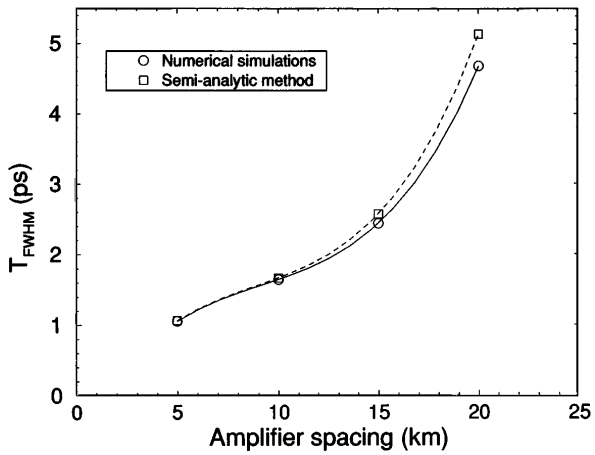

Fig. 5. Comparison of steady-state soliton widths for numerical simulations and the semianalytic model for some amplifier spacings.

As mentioned above, unlike in the average-soliton regime, in the quasi-adiabatic regime the soliton parameters changes considerably over one amplifier spacing. The condition of having a small amplifier spacing compared with the soliton period allows one to describe the propagation over many amplification stages by an averaged NSE for the average soliton.[3] In the quasi-adiabatic regime a nonlinear mapping of the soliton parameters seems to be more appropriate to analyze the soliton dynamics of a long chain of amplifiers.[16] Moreover, as shown above, the amplifier bandwidth has to be small to control the SSFS, suggesting the use of an accurate description of the amplification process (particularly for large amplifier spacings) as used in this paper.

In conclusion, we have analytically expressed two conditions for periodic amplification of short solitons (T_{FWHM} from 1 to 5 ps) and numerically solved this set of coupled nonlinear equations in terms of the soliton width and mean frequency for different amplifier spacings and gain bandwidths. Stable periodic short solitons are predicted as long as the dispersive waves are properly removed at every amplifier and provided that a gain or a filter of bandwidth comparable with the soliton spectral width is used to compensate for the soliton self-frequency shift. This approach may be applied to finding the soliton characteristics in a fiber laser having a significant frequency shift per round trip owing to intrapulse Raman scattering and a long-cavity configuration (several soliton periods).

ACKNOWLEDGMENTS

This research was supported by the Fonds pour la Formation de Chercheurs et l'Aide à la Recherche of the Québec Province Government (Canada) and by the U.S. Army Research Office.

REFERENCES

1. L. F. Mollenauer and K. Smith, "Demonstration of soliton transmission over more than 4000 km in fiber with loss periodically compensated by Raman gain," Opt. Lett. **13,** 675–677 (1988).
2. M. Nakazawa, H. Kubota, K. Kurokawa, and E. Yamada, "Femtosecond optical soliton transmission over long distances using adiabatic trapping and soliton standardization," J. Opt. Soc. Am. B **8,** 1811–1817 (1991); K. Rottwitt, J. H. Povlsen, and A. Bjarklev, "Long-distance transmission through distributed erbium-doped fibers," J. Lightwave Technol. **11,** 2105-2115 (1993).
3. A. Hasegawa and Y. Kodama, "Guiding-center soliton in optical fibers," Opt. Lett. **15**, 1443-1445 (1990); "Guiding-center soliton," Phys. Rev. Lett. **66,** 161–164 (1991).
4. L. F. Mollenauer, S. G. Evangelides, and H. A. Haus, "Long-distance soliton propagation using lumped amplifiers and dispersion-shifted fiber," J. Lightwave Technol. **9,** 194–197 (1991).
5. M. Nakazawa, K. Suzuki, H. Kubota, E. Yamada, and Y. Kimura, "Dynamic optical soliton communication," IEEE J. Quantum Electron. **26,** 2095–2102 (1990).
6. X. Tang and P. Ye, "Comparison of dynamic soliton communication and path-averaged soliton communication," Fiber Integ. Opt. **13,** 261–270 (1993).
7. B. A. Malomed, "Propagation of a soliton in a nonlinear waveguide with dissipation and pumping," Opt. Commun. **61,** 192–194 (1987).
8. S. M. J. Kelly, "Characteristic sideband instability of periodically amplified average soliton," Electron. Lett. **28,** 806–807 (1992).
9. A. E. Siegman, Lasers (University Science, Mill Valley, Calif., 1986), Chap. 28.
10. J. P. Gordon, "Theory of the soliton self-frequency shift," Opt. Lett. **11,** 662–664 (1986).
11. M. W. Chbat, P. R. Prucnal, M. N. Islam, C. E. Soccolich, and J. P. Gordon, "Long-range interference effects of soliton reshaping in optical fibers," J. Opt. Soc. Am. B **10,** 1386–1395 (1993).
12. K. Tai, A. Hasegawa, and N. Bekki, "Fission of optical solitons induced by stimulated Raman effect," Opt. Lett. **13,** 392–394 (1988).
13. R. Vallée and R.-J. Essiambre, "Long-distance soliton transmission with a nonlinear twin-core fiber," Opt. Lett. **19,** 2095–2097 (1994).
14. M. Matsumoto, H. Ikeda, and A. Hasegawa, "Suppression of noise accumulation in bandwidth-limited soliton transmission by means of nonlinear loop mirrors," Opt. Lett. **19,** 183–185 (1994).
15. J. P. Gordon and H. A. Haus, "Random walk of coherently amplified solitons in optical fiber transmission," Opt. Lett. **11,** 665–667 (1986).
16. B. A. Malomed, "Strong periodic amplification of solitons in a lossy optical fiber: analytical results," J. Opt. Soc. Am. B **11,** 1261–1266 (1994).
17. L. F. Mollenauer, J. P. Gordon, and S. G. Evangelides, "The sliding-frequency guiding filter: an improved form of soliton jitter control," Opt. Lett. **17**, 1575–1577 (1992).
18. G. P. Agrawal, *Nonlinear Fiber Optics*, 2nd ed. (Academic, Boston, Mass., 1995), Chap. 5.
19. K. J. Blow, N. J. Doran, and D. Wood, "Suppression of the soliton self-frequency shift by bandwidth-limited amplification," J. Opt. Soc. Am. B **5,** 1301–1304 (1988).